Summary of thesis entitled

Synthesis and Study of Conformationally Twisted Molecules and Chiral Roof Shape Amines

Thesis submitted to

The Maharaja Sayajirao University of Baroda

For the degree of

DOCTOR OF PHILOSOPHY

In

CHEMISTRY

Submitted by

Ms. Riddhi A. Gupta

Research Supervisor

Prof. Ashutosh V. Bedekar

Department of Chemistry
Faculty of Science
The Maharaja Sayajirao University of Baroda
Vadodara 390 002
Gujarat (INDIA)

February 2020

Synthesis and Study of Conformationally Twisted Molecules and Chiral Roof shape Amines:

Chapter 1: General Introduction:

Investigating the origin of chirality, revealed that the concept was introduced long ago by various well renowned scientists and researchers like *Archimedes of Syracuse* (250 B.C.), *Dominique Arge* (1811) and *Jean Baptiste Biot* (1835). But the understanding of the concept of chirality and its significance in chemistry was achieved by *Louis Pasteur* in 1848 who carried out recrystallization of sodium ammonium tartrate. *William Thomson* (Lord Kelvin) in 1893 proposed the modern definition of chirality *"I call any geometrical figure or group of points, chiral, and say that it possesses chirality, if its image in a plane mirror, ideally realized, cannot be brought to coincide with itself"* which is the universally accepted.

Application of chirality is not only restricted to synthetic organic chemistry, but the natural world around us is filled with structural motifs having an intrinsic handedness like *l*-amino acids, *d*-sugars, various flavours and fragrances *etc*. Chirality is extremely important in pharmaceutical industry as many drugs are chiral moieties containing one or more chiral centres differing in their pharmacological,[1] toxicological,[2] pharmacodynamic and pharmacokinetic properties.[3,4] Therefore, the synthesis of molecules in their enantiomeric forms and accurate analysis of the enantiopurity of such synthesized molecules has gained large impetus over recent years.

There are three main approaches for the preparation of chiral compounds: (1) Resolution of racemates usually involves the preferential crystallization of one diastereomeric species. Relatively rare (5-10%) is the crystallization of enantiomers having different crystal morphologies. (2) Chiral pool approach involves use of naturally available optically pure substrates, reagents or catalyst, inducing chirality in the product (3) Asymmetric Synthesis which involves the formation of a stereogenic centre under the influence of some external or internal chiral inducing agents. Having synthesized chiral compounds, the determination of its optical purity is carried out using various analytical techniques like HPLC or GC involving the use of chiral stationary phases,[5–7] mass spectrometry,[8–11] IR spectroscopy,[12] UV-Vis spectroscopy,[13] CD[14,15] & electrophoresis[16] *etc.*

UV-Visible spectroscopy is one of the most widely used tools for determination of enantiomeric purity due to its high sensitivity and simplicity to study various interactions. It is a useful that not only enables one to study the phenomena of molecular recognition, but also gives useful insights into the mode of interactions, the strength of complexation or

binding, as well as gives us the thermodynamic profile of complexation. However this method cannot be applied to substrates that are UV inactive. For such molecules, NMR spectroscopy is an efficient tool for determination of optical purity by involving the use of a chiral entity (CDA, CLSR or CSA) is required to convert the pair of enantiomers into diastereomers. **CDA** involves the derivatization of enantiomers by covalent bond formation with an enantiomerically pure compound leading to formation of diastereomers for the assay of enantiomeric purity. **CLSR** are usually six-coordinated lanthanide complexes of Eu, Pr[17,18] or Yb[19] which form a weak addition complex with a large variety of organic compounds. However, they suffer from various drawbacks like line broadening is observed if used in greater stoichiometric amounts as well as they are expensive which greatly limits their usefulness. **CSA**s interact with the analyte through non-covalent interactions such as dipole–dipole, ion-pairing, π-π interactions *etc*. Various NMR active nuclei[20] like ^{1}H, ^{19}F, ^{31}P, ^{13}C and ^{77}Se are used to study optical purity of analytes[21] owing to various advantages *e.g.* it is quick and simple to perform, with no problems of kinetic resolution or sample racemization provided that the complexes remain in solution, requires very low concentrations of host and guest and is very accurate for determination of optical purity as low as 1% *ee*.

Chapter 2: Introduction to small non-planar molecules:

The synthesis of small non-planar molecules pose synthetic challenges, they serve to test the limits of theoretical predictions and they provide insights into the effect of intramolecular strain on ground-state structures as well as internal mobility of electrons.[22] Such deformations can be bought about by forcing the bond angle deformations or the close proximity of bulky substituents leading to non-bonded repulsions and eclipsing strain. This is pronounced not only in heavily substituted benzenes, but also its analogues of naphthalene, phenanthrene and benzo[*c*]phenanthrene which have been individually discussed in following sections.

Section A: 1,8-Disubstituted Naphthalenes:

In naphthalene molecule, the substituents located at 1 and 8 position lie much closer to each other than the *ortho* placed substituents and are termed as *peri* positions. The placement of bulky substituents at these positions lead to deformation of the naphthalene skeleton from its planarity. Various 1,8-*tert*-butyl, diaroyl, diamide derivatives have been reported in literature with detectable enantiomerism at low temperatures. However only one report having 1,8-diadamantyl group has been isolated successfully in its enantiomerically pure

form, highlighting the difficulty in synthesis of such compounds.[23] We synthesized 1-(2,7-dihydroxynaphthalen-1-yl)ethan-1-one **(3)** by carrying out Fries rearrangement of naphthalene-2,7-diyl diacetate **(2)**. 69 was then subjected to bromination giving 1-(8-bromo-2,7-dihydroxynaphthalen-1-yl)ethan-1-one **(4)** as a single product (Scheme 1).

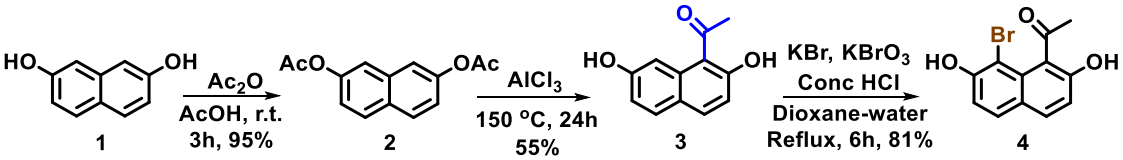

Scheme 1 Synthesis of 1-(8-bromo-2,7-dihydroxynaphthalen-1-yl)ethan-1-one (4)

SCXRD for 4 showed an interplanar angle of 4.58°. The main mode of relief of steric strain in the molecule was found to be the out of the plane deflection of the substituents at *peri* positions. In order to increase the rigidity of the molecule, we shifted our focus towards synthesis of naphthofuran **(6)** from the synthesized derivative **4** (Scheme 2).

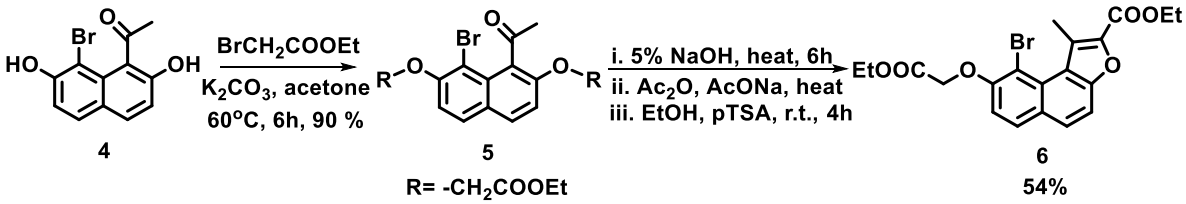

Scheme 2 Synthesis of naphthofuran derivative (6)

SCXRD for **6** showed an interplanar angle of 1.92°. This increase in planarity can be attributed to the less in plane angle of the furan ring as compared to that of the benzene ring. Hence for 1,8-substituted naphthalene, the major mode of steric strain relief is not the puckering of the aromatic rings, but the out of the plane deflection of the substituents present at the *peri* positions. This encouraged us to explore the next member of PAH series *i.e.* phenanthrenes.

Section B: 4,5-Disubstituted Phenanthrenes:

It has been reported, that for a given pair of substituents X, the internuclear distances for *peri* placed pairs would be greater than for *bay* (4^{th} and 5^{th} position of phenanthrene) placed pairs. Bulky substituents at these positions lead to optical isomerism in phenanthrenes if the substituents are bulky or large enough to prevent rapid interconversion of the enantiomers through a planar transition state. The effect of the bulkiness on the puckering of the phenanthrene moiety has been extensively studied by analysing the diastereotopic protons. We synthesized 4-bromo-3-hydroxyphenanthrene-9-carbonitrile **(16)** and attempted the synthesis of 4-bromo-3-hydroxy-5,7-dimethyl phenanthrene-9-carbonitrile **(17)** to compare the difference in the structural features due to the introduction of additional –Me group at

5th position. The electrophilic substitution of the phenolic precursors **(11** & **15)** to access the target molecules was the chosen pathway. The phenolic precursons were in turn obtained from the cyclization of corresponding stilbene derivatives **(9** & **13)** readily obtained from commercially available starting materials (Scheme 3 & 4).

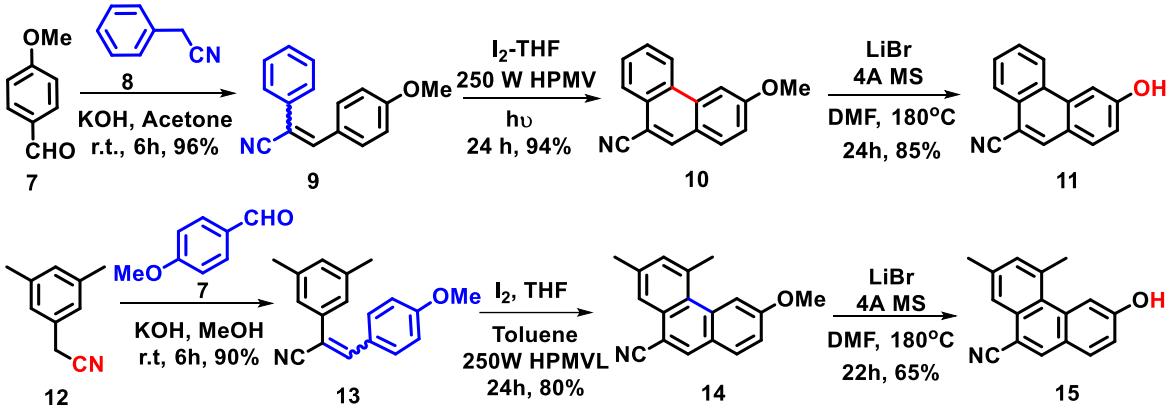

Scheme 3 Synthesis of phenanthrene from photocyclization of stilbene precursors

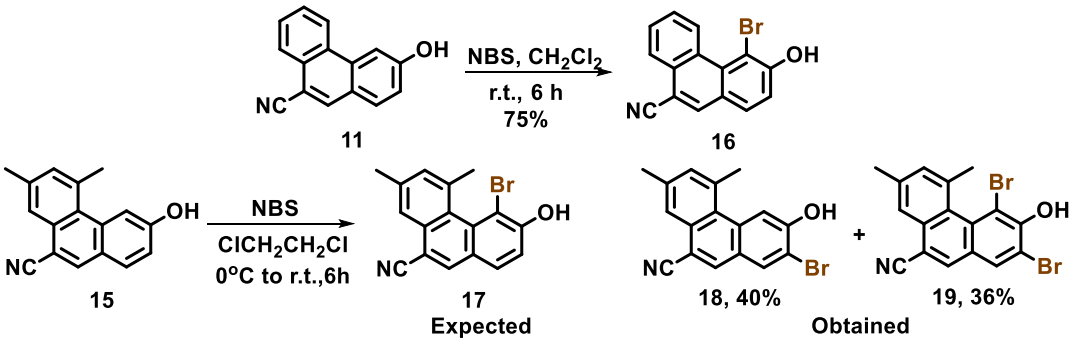

Scheme 4 Bromination of phenolic derivatives of phenanthrenes

We however failed to synthesize 4-bromo-3-hydroxy-5,7-dimethyl phenanthrene-9-carbonitrile **(17)**, but obtained a mixture of **18** and **19**. We also investigated the introduction of a smaller halogen atom *ie.* –Cl to modulate the size of the substituent at the 4th position of a 5-methyl phenanthrene motif. It was observed that chlorination of 3-hydroxy-5,7-dimethylphenanthrene-9-carbonitrile **(15)** indeed gave 4-chloro-3-hydroxy-5,7-dimethylphenanthrene-9-carbonitrile **(20)** as the only product (Scheme 5).

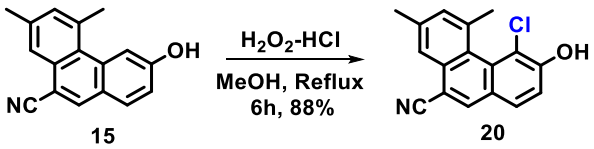

Scheme 5 Chlorination of 3-hydroxy-5,7-dimethylphenanthrene-9-carbonitrile (15)

All the derivatives synthesized were subjected to ether formation with *p*-bromo benzyl bromide to test for the diastereotopic nature of the benzylic protons.

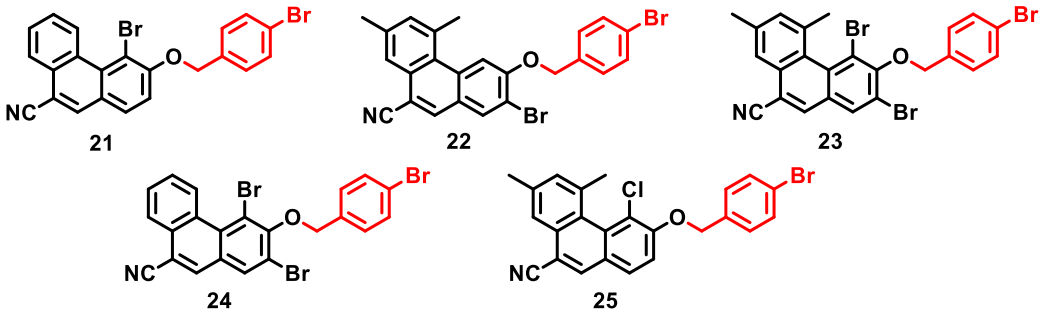

Figure 1 Ether derivatives synthesized under present study

Among all the derivatives synthesized, **23** & **25** showed two doublets for the benzylic protons which supports the hypothesis that they exist in two enantiomeric forms in NMR time scale. However, these derivatives could not be separated using chiral HPLC, which shows that the enantiomers rapidly interconvert at room temperature. This motivated us to introduce a fourth benzene ring fused to the phenanthrene core leading us to synthesize benzo[*c*]phnanthrenes.

Section C: 1-Substituted Benzo[*c*]phenanthrenes (B[*c*]Ph):

Steric interference due to substituents at positions 1 and 12 leads to the increased deformation of the rings which would affect the physical and chemical properties of B[*c*]Ph. However, only a few compounds of 1-substituted B[*c*]Ph derivatives have been studied because of their unavailability due to difficulties in synthesis. None of the 1-substitued B[*c*]Ph derivatives have been resolved due to low barrier of racemization facilitating rapid interconversion of the enantiomers in solution.

Hence we took up this objective and synthesized a series of 1-Me and 1-Br B[*c*]Ph derivatives by photocyclization of the corresponding naphthastilbenes. We also introduced –CN group and varied its position on the B[*c*]Ph motif to analyse the difference in their crystal packing and other non-covalent interactions. The formation of 1,3-dimethyl B[*c*]Ph derivatives occurred readily with formation of the target molecules **(26-28)** as the sole product. However, the photocyclization of bromo bearing naphthastilbenes lead to the formation of a large number side products which were carefully separated using extensive column chromatography. We were able to isolate 1-bromo B[*c*]Ph derivatives **(29-31)** in moderate yields. All the synthesized derivatives were subjected to SCXRD analysis (Table 1 & 2).

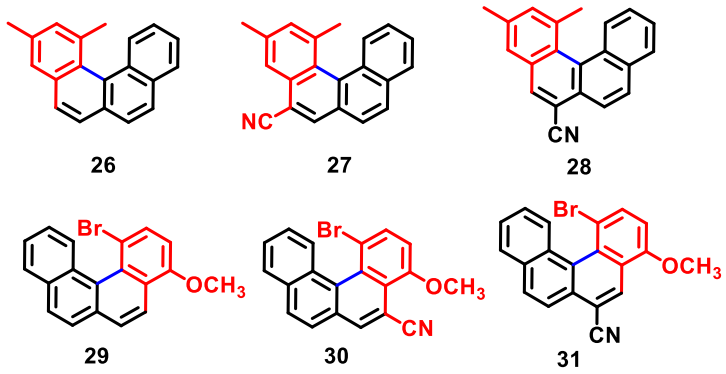

26 27 28 29 30 31

Figure 2 Synthesized B[*c*]Ph derivatives (26-31)

Table 1 Comparison of structural features for 1,3-dimethyl B[*c*]Ph derivatives

		Compound 27	**Compound 28**	**Compound 26**
Space group		P21 21 21	Pī	Pn21a
Interplanar angles	A & B	13.53°	14.07°	13.40°
	B & C	14.67°	13.85°	13.88°
	C & D	13.81°	10.87°	10.14°
	A & D	41.81°	37.85°	36.72°
Torsional Angle	C1-C17-C15-C13	30.79°	32.40°	32.08°
	C17-C15-C13-C12	21.15°	16.64°	15.00°
	Sum	51.94°	49.04°	47.08°

Table 2 Comparison of structural features for 1-bromo B[*c*]Ph derivatives

		Compound 30	**Compound 31**	**Compound 29**
Space group		P21/c	P21/c	Pn21a
Interplanar angles	A & B	13.86°	11.27°	14.33°
	B & C	16.33°	13.77°	13.83°
	C & D	13.00°	13.70°	12.34°
	A & D	42.55°	38.66°	40.04°
Torsional Angle	C1-C17-C15-C13	33.97°	28.31°	30.21°
	C17-C15-C13-C12	16.98°	19.81°	19.15°
	Sum	50.95°	48.12°	49.36°

The structural features of these derivatives have been compared and it was concluded that the crystal packing is strikingly different in all the derivatives under study.

Our next objective was to prove the existence of these molecules in two enantiomeric forms namely *P* and *M*. The three 1,3-dimethyl B[*c*]Ph derivatives **(26-28)** synthesized showed a broad peak at room temperature which was effective resolved to almost base line separation under cryogenic conditions (-20°C). The 1-bromo B[*c*]Ph **(29-31)** derivatives however, showed two well resolved peaks at room temperature itself due to high barrier of enantiomerization causing the two enantiomers to be stable at room temperature, making them ideal candidates for attempting resolution.

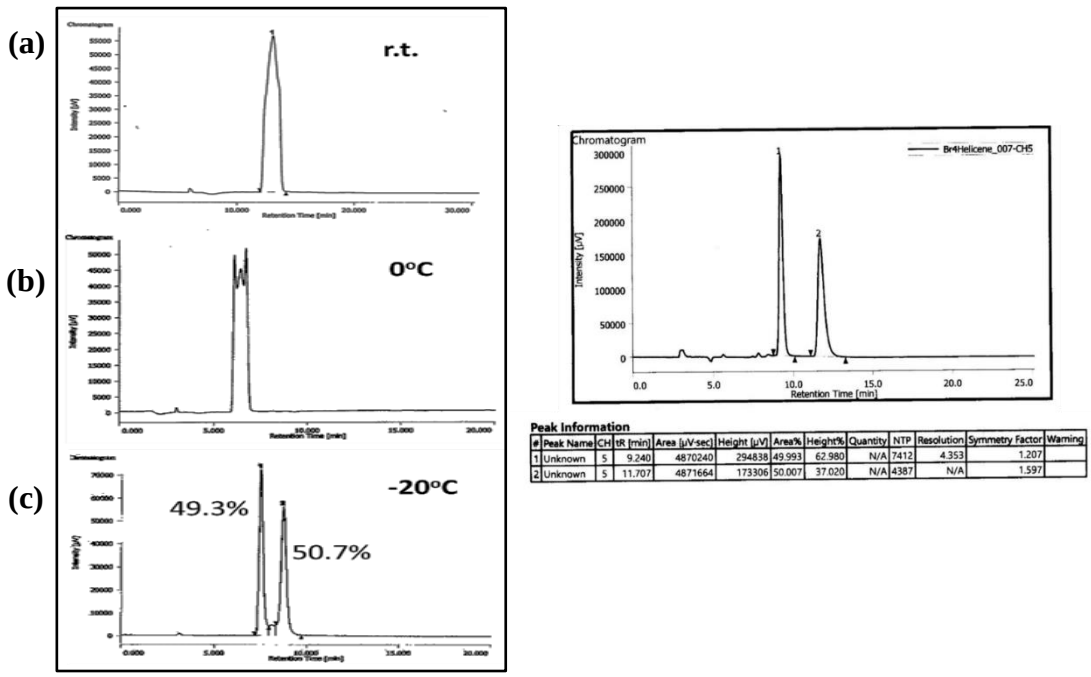

#	Peak Name	CH	tR [min]	Area [μV·sec]	Height [μV]	Area%	Height%	Quantity	NTP	Resolution	Symmetry Factor	Warning
1	Unknown	5	9.240	4870240	294838	49.993	62.980	N/A	7412	4.353	1.207	
2	Unknown	5	11.707	4871664	173306	50.007	37.020	N/A	4387	N/A	1.597	

Figure 3 HPLC chromatogram of 1,3-dimethylB[*c*]Ph-5-carbonitrile (27) (left) and 1-bromo-4-methoxyB[*c*]Ph-6-carbonitrile (31) (right)

Spontaneous Deracemization:

When racemic compounds are subjected to crystallization without the addition of external chiral moieties, only 5-10% of them crystallize as *conglomerate* where each crystal contains only one of the enantiomers leading to spontaneous resolution. The crystals may differ in morphology and can be handpicked into pure enantiomers giving a maximum yield of 50%. Sometimes, it is possible to racemize the other isomer in a separate loop and reinjecting the racemized mixture in the resolution process repeatedly causing preferential crystallization of one enantiomer only. Such a resolution leads to complete conversion of the racemate to one enantiomer leading to possibility of 100% theoretical yield and is termed as *'Spontaneous Deracemization'*.[24] To determine if such spontaneous deracemization has taken place, we utilized single crystal X-ray diffraction studies along with CD spectroscopy. Among the six synthesized derivatives **(26-31),** only **27** showed this phenomena where needle like crystals were obtained from a mixture of hexane-ethyl acetate or hexane-acetone mixture. The crystals were separated from both the solvent mixtures independently, and subjected to SCXRD analysis. The compound crystallized in a chiral $P2_12_12_1$ space group possessing four molecules present in a unit cell having the same configuration. However the configuration of the molecules in the crystals obtained from hexane-ethyl acetate was opposite to those obtained from hexane-acetone mixture. Both the samples were subjected to solid state CD analysis. The CD spectra for the crystals obtained from hexane-ethyl

acetate was a bisignate with a curve at higher wavelength being positive and that at lower wavelength being negative. Hence, the absolute configuration obtained from solid state CD was assigned as "*P*" which is in agreement with that assigned using the Flack parameter. CD spectra for the crystals obtained from hexane-acetone showed an almost equal and opposite bisignate curve, confirming that these crystals constituted the other isomer *M*.

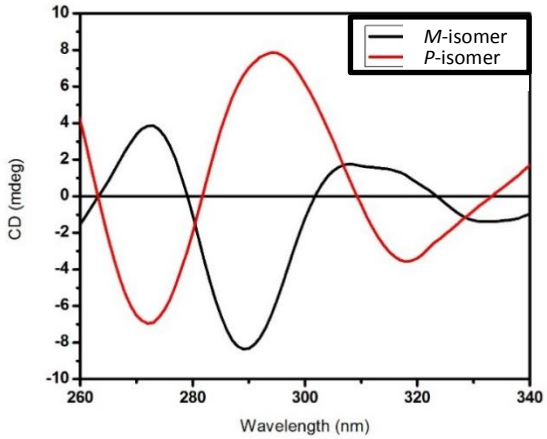

Figure 4 Solid state CD spectra of both the isomers

The reproducibility of these results was confirmed by carrying out SCXRD for 6 samples of crystals obtained from hexane-ethyl acetate mixture and 3 samples from hexane-acetone while more are being screened presently. In all the cases, the yield of the crystals obtained was >80% indicating the role of spontaneous deracemization in this molecule. As these molecules undergo rapid racemization in solution state, the optical rotation for this compound was not obtained and hence these enantiomers could only be characterized using SCXRD and solid state CD measurements.

Chapter 3: Synthesis and Study of 5,13-dicyano oxa[7]helicene and helicene-like molecules:

Helicenes are analogues of phenanthrene formed as a result of *ortho* fusion of four or more aromatic systems. The intramolecular steric repulsion between the π-systems of the terminal rings in helicenes leads to conformational distortion causing loss of planarity rendering the molecule to adapt a helical topology. If the helical twist is right handed (or clockwise) it is denoted by *P* while a left handed (anticlockwise) helical twist is denoted by *M*.[25] The incorporation of furan ring into the helicene skeleton are classified as oxahelicenes. Due to the difficulty in the synthesis of oxahelicenes, they have been relatively less explored. Numerous strategies have been developed to embed furan ring in helicene skeleton. The cyclization of BINOL type derivative is the methodology of choice as it provides a handle for effective separation during the synthesis to obtain the target helicenes as pure

enantiomers. To synthesize oxa[7]helicene motif **(34)**, we accessed bis-phenanthrol **(32)** (analogue of BINOL) by oxidative C-C coupling of phenanthrol **(11)** synthesized earlier The activation of –OH group by nonaflate followed by Pd-catalysed Buchwald-Hartwig reaction (Scheme 6) lead to the formation of our target helicene **(34)** in moderate yield.

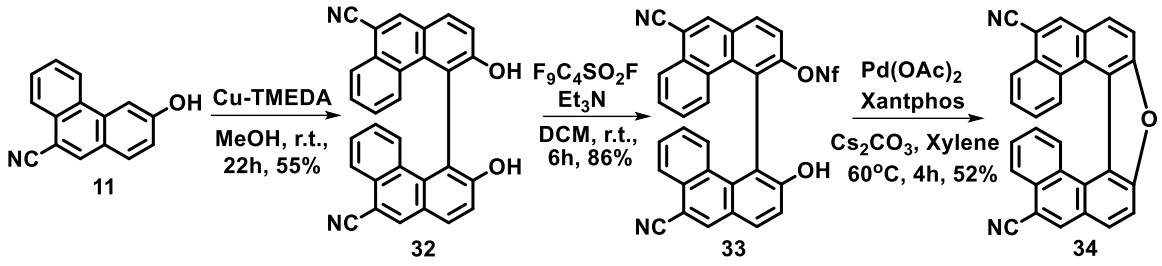

Scheme 6 Synthesis of 6,13-dicyano oxa[7]helicene (34)

The other class of helicene-like compounds diarylated[*d*,*f*][1,3]dioxepine analogue was also synthesized by subjecting the bis-phenanthrol **(32)** to ether formation with diiodomethane and Cs_2CO_3 as base (Scheme 7).

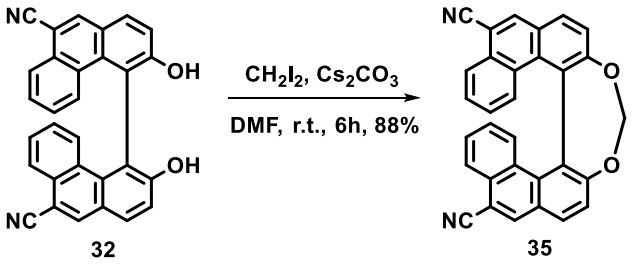

Scheme 7 Synthesis of helicene-like diarylated[*d*,*f*][1,3]dioxepine (35)

To access these target compounds in their enantiomerically pure forms, the bis-phenanthrol **(32)** was subjected to resolution *via* diastereomer formation with (-)-menthyl chloroformate (Scheme 8). The diastereomeric bis-carbonate **(32)** hence obtained, was subjected to crystallization using 30% chloroform in hexane giving transparent clear crystals of **(*S*)-36** in 99%*de* and concentration of mother liquor gave **(*R*)-36** in 96%*de*. The separated diastereomers were then subjected to mild basic hydrolysis to access both the enantiomers of 3,3'-dihydroxy[4,4'-biphenanthrene]-9,9'-dicarbonitrile **(32)**.

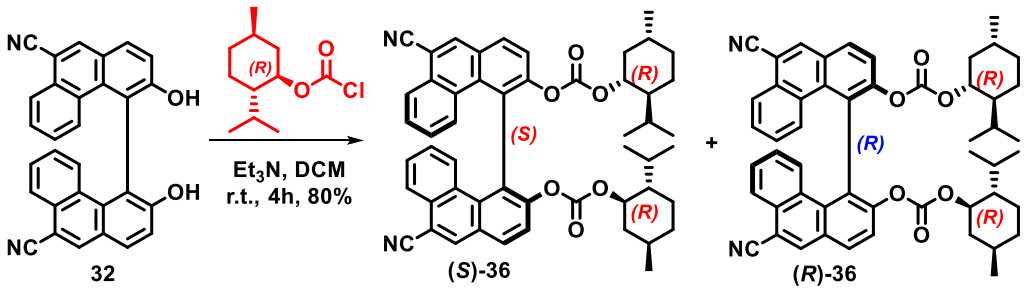

Scheme 8 Synthesis of diastereomeric bis-carbonate using chiral auxiliary

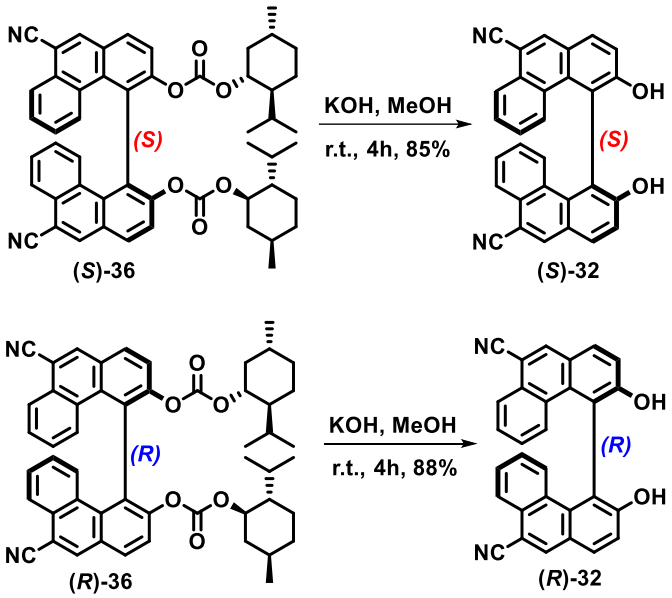

Scheme 9 Regeneration of optically pure 32

The optical purity of **32** after basic hydrolysis of the bis-carbonate derivative **(*S*)-36** & **(*R*)-36** was analysed using chiral HPLC which confirmed **(*S*)-32** is in 99%*ee* and **(*R*)-32** in 96%*ee*. Each enantiomer of 3,3'-dihydroxy[4,4'-biphenanthrene]-9,9'-dicarbonitrile **(32)** was subjected to same reaction conditions to obtain our target 5,13-dicyano-9-oxa[7]helicene **(34)** and helicene-like **(35)** in enantiomerically pure form without any racemization.

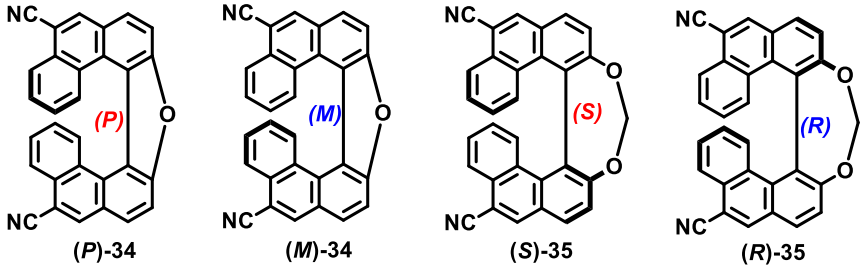

Figure 5 Synthesis of helicene and helicene-like compounds in optically pure form

The SCXRD for oxa[7]helicene **(34)** showed characteristic lowering of C-C bond lengths at outer rim of the helical core, while that on the inside rim were found to be slightly elongated in comparison to normal aromatic system. The angle between the planes passing through the two terminal rings was found to be 39.64° and the sum of five dihedral angles on the inner helical rim was 76.8°. The addition of –CN group lead to substantial increase in the interplanar angle of the helicene when compared to unsubstituted oxa[7]helicene which is a key aspect in its potential application in various fields of chemistry.

The comparison of SOR for the present set of compounds indicated that both the isomers of chirally pure **32** showed much less rotation, which changed considerably when converted to

helicene-like compound **35**. When the helical compound **34** was synthesized, there was considerable increase in the value of optical rotation as well as molecular rotation (Table 3).

Table 3 Chiroptical properties of isomers of 32, 34 and 35

	(*R*)-**32**	(*S*)-**32**	(R_a)-**35**	(S_a)-**35**	(*M*)-**34**	(*P*)-**34**
$[\alpha]^a$	-150	+157	-515	+543	-755	+790
$[\Phi]^b$	-655	+685	-2310	+2433	-3160	+3306

[a]Specific optical rotation, c = 0.1, in DMSO; [b]Molecular optical rotation;
(*R*)-**32**, (R_a)-**35** and (*M*)-**34** = 96% *ee*; (*S*)-**32**, (S_a)-**35** and (*P*)-**34** = 99% *ee*

A comparison of UV-Vis and fluorescence spectroscopy of **34** and **35** showed that the longest absorption maxima weas observed at 323 and 310 nm respectively (Figure 6). The replacement of furan unit with dioxapine unit in the helical skeleton lead to a blue shift of 13 nm which may be attributed to the break in effective conjugation of the molecule due to the presence of an sp^2 carbon bridge (Table 4). The lower value of the emission maxima and Strokes shift in helicenes is probably attributed to loss in energy due to more facile intersystem crossing in such molecules (Figure 6).[26]

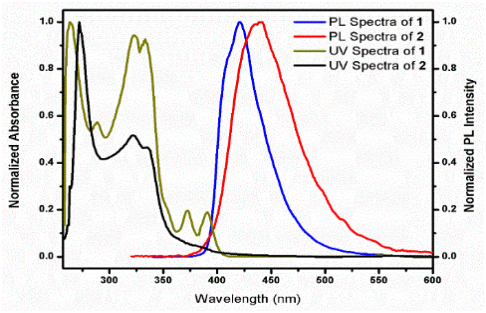

Table 4 Photophysical properties of 34 & 35

Compound	λ_{abs} (nm)	λ_{ems} (nm)	Stokes Shift (nm)
34	323	421	98
35	310	439	129

Figure 6 Absorption and Emission Spectra of 34 & 35 in DMSO (abs 1.5X10^{-6} M; ems 1X10^{-4} M)

The separated isomers of **34** and **35** were also analysed by CD where two opposite bisignate couplets showing opposite cotton effects, were observed (Figure 7).

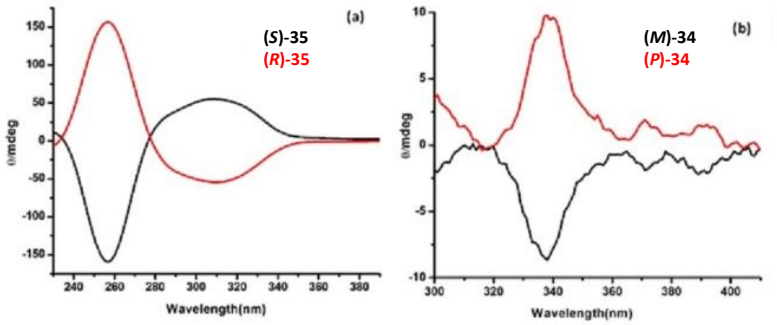

Figure 7 CD spectra of (a) (Black) (*S*)-35 and (Red) (*R*)-35 (2.4 X 10^{-4}M, $CHCl_3$) (b) (Red) (*P*)-34 and (Black) (*M*)-34 (2.1 X 10^{-4}M, DMSO) at 25°C

The isomer of **34** showing a positive curve at the higher wavelength was assigned (*P*) and that with a negative curve was assigned as (*M*) configuration. For **34**, the CD band appears at a wavelength of 340 nm and that for **35** is 260 nm owing to the difference in their dihedral angles

The helical topology and extended π-conjugation make helicenes a class of chromophoric compounds suitable for the study of their CPL activity which is the differential absorption of left and right circularly polarized light, quantified by the luminescence dissymmetry factor g_{lum}. Both, (*P*)-/(*M*)-**34** and (*R*)-/(*S*)-**35**, showed a somewhat mirror-like CPL signal with opposite g_{lum} values around the emission maximum (+0.003/–0.002 and +0.005/–0.002, respectively) which is in the typical range of g_{lum} values for most chiral organic molecules.[27]

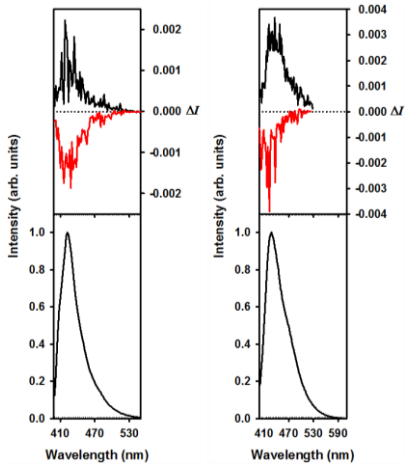

Figure 8 CPL (upper curve) and total luminescence (lower curve) spectra of (*P*)-/(*M*)-34 (left) and (*R*)-/(*S*)-35 (right)

Such molecules having unique structure and properties due to their helical morphology are opening the door to a new world. The synthesis and resolution of helicenes mentioned in this work, could also be a contributing guideline and projection of helicenes in future.

Chapter 4: Synthesis and Application of Roof shape Secondary Amines as CSA:

Diels-Alder reaction of anthracene with s dienophiles lead to the formation of compounds possessing shape that closely resembles to that of a roof of a house has led to term this class of compounds as '*Roof shaped*' compounds. These compounds possess bulkiness and molecular rigidity due to its basic skeleton and functional groups attached to the bridge of the molecular architecture. Various roof shape compounds have been known to act as clathrate hosts and have been studied for their inclusion behaviour,[28] as precursors for liquid chromatographic chiral stationary phases,[29,30] ligands in asymmetric synthesis[31,32] *etc.* Earlier our group has reported chiral cyclic tertiary amines and scanned them as CSAs

for discrimination of the signals of some optically active compounds using NMR spectroscopy.[33,34] Roof shape alcohol was also used as chiral auxiliary for optical enrichment of α-halo acids.[35]

Section A: Effect of additional chirality on molecular recognition:

We have explored the effect of introducing another aromatic system by choosing to attach benzyl amine with the aim of adding an additional supramolecular interaction in the form of π-stacking. In order to study the match-mismatch effect we further prepared two derivatives by selecting two enantiomers of the chiral benzyl amine (Scheme 10).

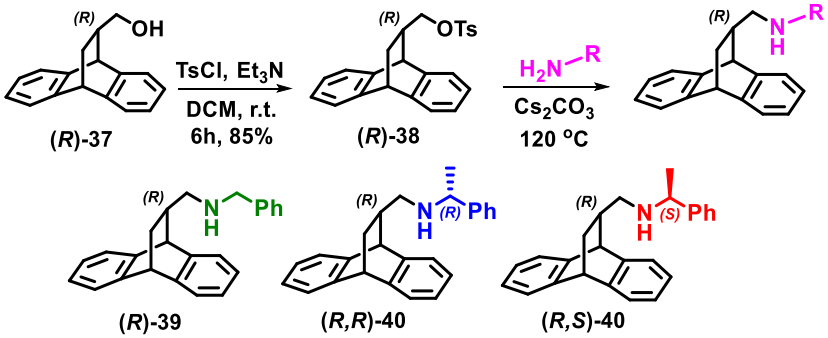

Scheme 10 Synthesis of roof shape chiral secondary amines (39 & 40)

Having prepared the three roof-shape secondary amines **(*R*)-39**, **(*R*,*R*)-40** and **(*R*,*S*)-40**, we examined different acidic substrates for a possible and detectable discrimination of the NMR signals in $CDCl_3$ (400 MHz; 20 mM concentration; ratio of 1:1).

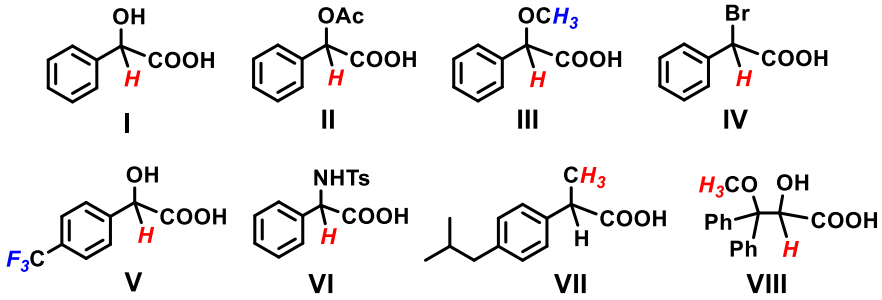

Table 5 Comparison of the ability of CSA to discriminate signals of chiral acids

No	Substrates	NMR nucleus	(*R*)-**39**		(*R*,*R*)-**40**		(*R*,*S*)-**40**	
			$\Delta\delta^a$	$\Delta\Delta\delta^b$	$\Delta\delta$	$\Delta\Delta\delta$	$\Delta\delta$	$\Delta\Delta\delta$
1	**I**	^{1}H	-0.411	0.123	-0.285	0.093	-0.289	--^{c}
2	**II**	^{1}H	-0.130	0.050	0.003	0.032	-0.041	--^{c}
3	**III**	^{1}H (Cα) ^{1}H (CH_3)	-0.179 -0.167	0.028 0.003	-0.055 0.060	0.043 0.049	-0.104 -0.082	--^{c} --^{c}
4	**IV**	^{1}H	-0.010	0.034	0.128	0.040	0.020	--^{c}

5	**V**	^{1}H ^{19}F	-0.351 -0.127	0.077 0.032	-0.356 -0.094	0.062 0.076	-0.357 -0.099	0.017 0.015
6	**VI**	^{1}H (Cα) ^{1}H (CH_3)	-0.165 -0.396	0.055 0.079	-0.201 -0.353	0.070 0.074	-0.146 -0.287	0.049 0.031
7	**VII**	^{1}H	-0.038	0.015	0.007	0.019	-0.004	0.008
8	**VIII**	^{1}H (Cα) ^{1}H (OCH_3)	-0.135 -0.029	0.039 0.016	-0.067 0.020	0.146 0.079	-0.056 0.028	0.006 0.013

[a]Induced chemical shift (Δδ); [b]Nonequivalence (ΔΔδ); [c]Signals were not separated

Since our present secondary amine based roof-shape CSAs were expected to be strongly basic in nature, we investigated them for their ability to interact with weakly acidic BINOL or its derivatives.

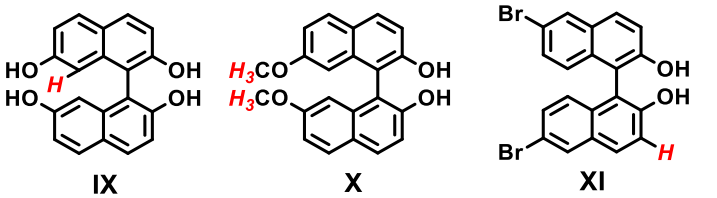

Table 6 Comparison of ability of CSA to discriminate signals of chiral BINOL derivatives

No	Substrates	NMR nucleus	(*R*)-**39**		(*R*,*R*)-**40**		(*R*,*S*)-**40**	
			Δδ[a]	ΔΔδ[b]	Δδ	ΔΔδ	Δδ	ΔΔδ
1	**IX**	^{1}H	-0.015	0.019	0.005	--[c]	0.017	0.032
2	**X**	^{1}H	-0.008	0.004	-0.004	0.005	-0.003	0.002
3	**XI**	^{1}H	0.005	0.011	0.001	0.018	-0.002	0.005
4	**XII**	^{1}H	0.002	--[c]	0.001	--[c]	--[d]	--[c]
5	**XIII**	^{1}H	-0.033	--[c]	-0.014	--[c]	-0.014	0.007
6	**XIV**	^{31}P	+0.529	0.205	-0.114	--[c]	-0.739	0.341

[a]Induced chemical shift (Δδ); [b]Nonequivalence (ΔΔδ); [c]Signals were not separated

Hence, **(*R,S*)-40** proved to be slightly superior class of CSA for binaphthyl system, while its diastereomer **(*R,R*)-40** was found more effective in the chiral recognition of derivatives of mandelic acid. Such a match−mismatch effect for controlling supramolecular interactions between diastereomeric chiral solvating agents for molecular recognition is noteworthy. The

SCXRD analysis for diastereomeric salts of **(*R,R*)-40** with *R*-MA and **(*R,R*)-40** with *S*-MA were analysed. For **(*R,R*)-40.*R*-MA** salt, the hydrogen attached to the chiral carbon of (*R*)-MA appears to be laying on top of one of the aromatic rings of the roof-shape bicyclic framework. The shortest perpendicular distance between the plane passing through this ring and the hydrogen is 4.18 Å, and it is observed to be shifting upfield region due its shielding effect in ^{1}H NMR analysis. No such interaction was seen for the other diastereomeric pair **(*R,R*)-40.*S*-MA** clearly showing the role of orientation of the second chiral center on molecular recognition.

Section B: Electronic effects on molecular recognition:

It has been reported that the presence of various electron withdrawing or releasing substituents on a molecule, is the prime factor affecting the phenomena of molecular recognition.[36] Since the electron accepting strength of -NO_2 group and electron donating strength of –OCH_3 group is one of the strongest, we selected these substituents to occupy 4-position of the benzyl moiety utilizing reductive amination methodology.

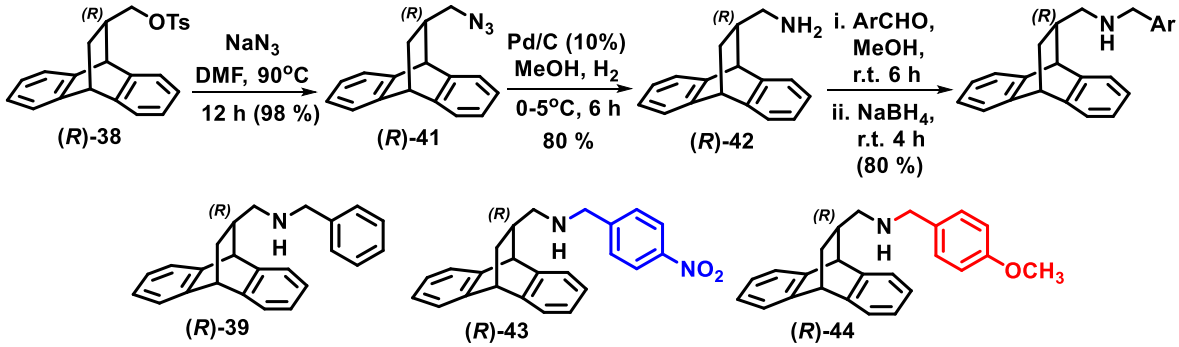

Scheme 11 Synthesis of chiral roof shape amines using reductive amination method

The synthesized roof shape amines were then screened to compare their ability of molecular recognition of chiral acids by recording ^{1}H NMR of equimolar mixture of CSA and test acid in $CDCl_3$ (400 MHz; 20 mmol).

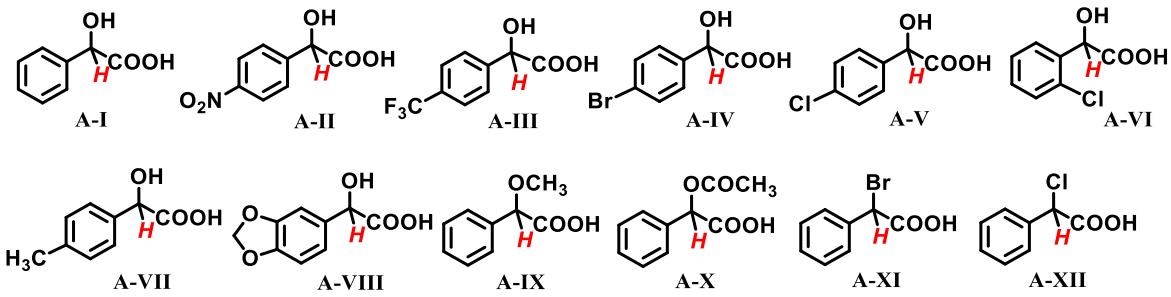

Table 7 Comparison of the ability of CSA to discriminate C$_\alpha$*H* signals of chiral acids[a]

No	Substrate	(*R*)-**39**		(*R*)-**43**		(*R*)-**44**	
		Δδ	ΔΔδ	Δδ	ΔΔδ	Δδ	ΔΔδ
1	**A-I**	-0.431	0.123	-0.379	0.146	-0.253	0.037
2	**A-II**	-0.405	--[b]	-0.343	0.014	-0.425	0.005
3	**A-III**	-0.351	0.077	-0.284	0.022	-0.371	0.041
4	**A-IV**	-0.346	0.004	-0.312	0.042	-0.288	--[b]
5	**A-V**	-0.429	0.008	-0.386	--[b]	-0.342	0.007
6	**A-VI**	-0.285	0.034	-0.305	0.064	-0.350	0.058
7	**A-VII**	-0.421	0.010	-0.327	0.042	-0.418	0.014
8	**A-VIII**	-0.336	0.027	-0.404	0.119	-0.457	0.092
9	**A-IX**	-0.179	0.028	-0.164	0.021	-0.130	0.015
10	**A-X**	-0.130	0.050	-0.195	0.029	-0.153	0.040
11	**A-XI**	-0.010	0.034	-0.011	0.016	-0.003	0.017
12	**A-XII**	-0.092	0.003	-0.068	--[b]	-0.087	0.025

[a] In $CDCl_3$ (20mM), [b] Not resolved

The exploration of ability of molecular recognition was then extended to *N*-tosyl amino acids as they are important synthetic blocks in medicinal and allied chemistry, hence the determination of their optical purity is critical.

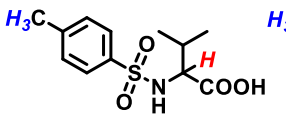

AA-I

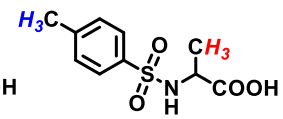

AA-II

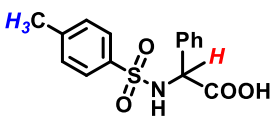

AA-III

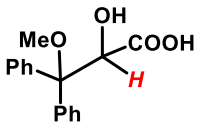

B-I

Table 8 Discrimination of *N*-Ts amino acids **AA-1** to **AA-III** and **B-I**[a]

No	Substrate	**NMR nuclei**	(***R***)-**39**		(***R***)-**43**		(***R***)-**44**	
			Δδ	**ΔΔδ**	**Δδ**	**ΔΔδ**	**Δδ**	**ΔΔδ**
1	**AA-I**	Cα*H*	+0.623	0.087	+0.832	0.145	+1.062	0.168
		Ar-C*H*$_3$	-0.226	0.012	-0.159	0.018	-0.249	0.017
2	**AA-II**	CαC*H*$_3$	-0.074	0.012	-0.102	0.018	-0.074	0.013
		Ar-C*H*$_3$	-0.169	--[b]	-0.123	0.008	-0.074	0.013
3	**AA-III**	Cα*H*	-1.063	0.055	--[c]	--[c]	-1.101	0.056
		Ar-C*H*$_3$	-0.154	0.021	--[c]	--[c]	-0.168	0.015
4	**B-I**	Cα*H*	-0.135	0.039	-0.028	0.003	-0.173	0.050

[a] In $CDCl_3$ (20mM), [b] Not resolved, [c] precipitation observed

UV-Visible spectroscopy was utilized to study the host-guest binding by observing the change in absorbance of all the hosts (fixed concentration) with increase in concentration of

each enantiomer of *R*-/*S*-**A-I** or *D*-/*L*-**AA-I**. The association constants (K_R and K_S for **A-I** or K_L and K_D for **AA-I**) and correlation coefficients (R) were determined by using modified Benesi-Hildebrand equation (plot of 1/ΔA versus 1/[G]) summarized in (Table 9 & 10).

Table 9 Association constant K for UV response with CSAs

Substrate	(*R*)-39	(*R*)-43	(*R*)-44
(*R*)-**A-I**	257.0694	909.0909	140.2525
(*S*)-**A-I**	251.2563	826.4463	65.0195
(*D*)-**AA-I**	1895.6843	2601.5448	4931.5428
(*L*)-**AA-I**	1132.1656	1582.8871	3306.7908

Table 10 Gibbs free energy (ΔG)[a] of CSAs with isomers of substrates

Substrate	(*R*)-39	(*R*)-43	(*R*)-44
(*R*)-**A-I**	-13.7558	-16.8868	-12.2539
(*S*)-**A-I**	-13.6991	-16.6506	-10.3483
(*D*)-**AA-I**	-18.7085	-19.4931	-21.0784
(*L*)-**AA-I**	-17.4308	-18.2615	-20.0877

[a]Calculated with ΔG = - RT lnK

The results of binding study were in accordance with the conclusions drawn by NMR experiments (Table 7 and 8) where **(*R*)-58** showed the best recognition towards **A-I** and **(*R*)-59** showed the best results with **AA-I**.

Section C: Effect of distance of chiral center on chiral recognition:

Another parameter that greatly affects the chiral discrimination ability of a host, is the distance of the chiral center from the group undergoing binding interactions. In all the CSAs under study, the primary site of interaction is one sp^3 carbon away from the chiral center, providing some amount of molecular flexibility to the molecule. In order to make the amines conformationally more rigid, we focused our synthesis towards a chiral roof shape secondary amine where the amino group is directly attached to the chiral center of the roof shape moiety and compare their CSA activity.

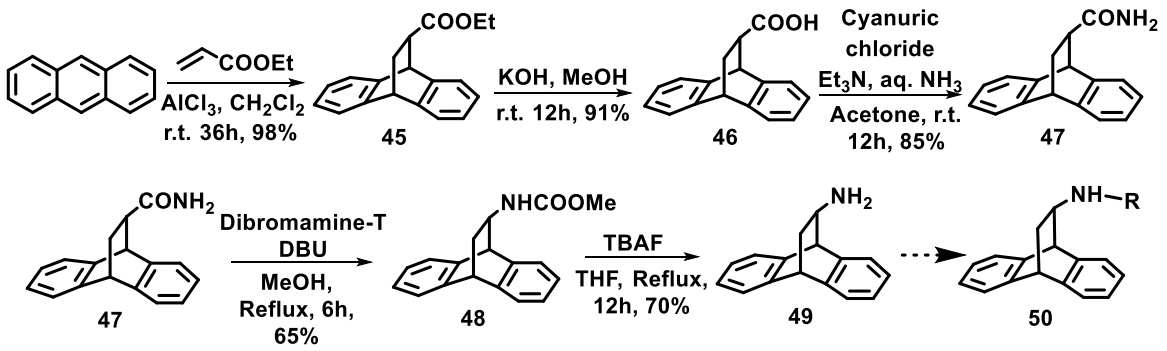

Scheme 12 Synthetic Scheme to access amine 49

To resolve racemic-**49**, (*R*)-menthyl chloroformate was the reagent of choice for the formation of diastereomeric carbamate (Scheme 13).

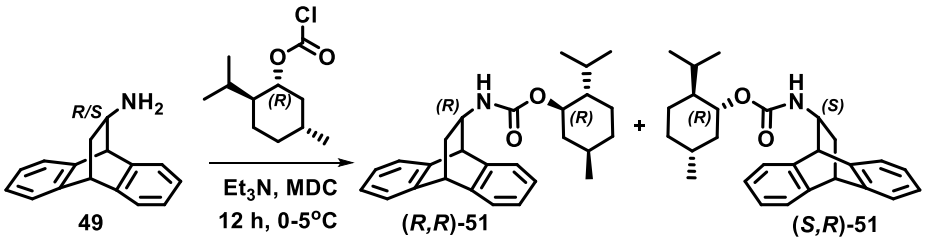

Scheme 13 Resolution of amine 49 by forming diastereomeric menthyl carbamate

Slow evaporation of a solution of the mixture from hexane lead to the crystals of **(*R*,*R*)-51** in 99.9% *de* which was confirmed by SCXRD and chiral HPLC analysis. The synthesis of CSAs is underway.

References:

[1] M. Kiran, P. Yadav, P. Deolekar, V. Thakre, *Int. J. Pharm. Res. Allied Sci.* **2012**, *1*, 7–10.

[2] S. W. Smith, *Toxicol. Sci.* **2009**, *110*, 4–30.

[3] A. M. Evans, *Eur. J. Clin. Pharmacol.* **1992**, *42*, 237–256.

[4] D. R. Brocks, R. Mehvar, *Clin. Pharmacokinet.* **2003**, *42*, 1359–1382.

[5] W. H. Pirkle, Y. Liu, *J. Chromatogr. A* **1996**, *736*, 31–38.

[6] G. K. E. Scriba, *J. Chromatogr. A* **2016**, *1467*, 56–78.

[7] C. Cagliero, B. Sgorbini, C. Cordero, E. Liberto, P. Rubiolo, C. Bicchi, *Isr. J. Chem.* **2016**, *56*, 925.

[8] M. T. Reetz, M. H. Becker, H.-W. Klein, D. Stockigt, *Angew. Chem. lnt. Ed.* **1999**, *38*, 1758–1761.

[9] J. Guo, J. Wu, G. Siuzdak, M. G. Finn, *Angew. Chem. lnt. Ed.* **1999**, *38*, 1755–1758.

[10] C. Markert, A. Pfaltz, *Angew. Chemie Int. Ed.* **2004**, *43*, 2498–2500.

[11] X. Yu, Z.-P. Yao, *Anal. Chim. Acta* **2017**, *968*, 1–20.

[12] M. T. Reetz, M. H. Becker, K. M. Kühling, A. Holzwarth, *Angew. Chem. lnt. Ed.* **1998**, *37*, 2647–2650.

[13] W. Cui, W. Guang, S. Zhang, J. Fan, X. Yin, M. Li, S. Choon, *Biosens. Bioelectron.* **2009**, *25*, 488–492.

[14] M. W. Ghosn, C. Wolf, *J. Am. Chem. Soc.* **2009**, *131*, 16360–16361.

[15] S. Nieto, J. M. Dragna, E. V Anslyn, *Chem. Eur. J.* **2010**, *16*, 227–232.

[16] A. Electrophoresis, M. T. Reetz, K. M. Kühling, A. Deege, H. Hinrichs, D. Belder, *Angew. Chem. lnt. Ed.* **2000**, *39*, 3891–3893.

[17] R. R. Fraser, M. A. Petit, M. Miskow, *J. Am. Chem. Soc.* **1972**, *94*, 3253–3254.

[18] M. Kainosho, K. Ajisaka, W. H. Pirkle, S. D. Beare, *J. Am. Chem. Soc.* **1972**, *94*, 5924–5926.

[19] A. Tangerman, B. Zwanenburg, *Recl. des Trav. Chim. des Pays-Bas* **1977**, *96*, 196–199.

[20] F. Balzano, G. Uccello-Barretta, F. Aiello, *Chiral Anal.* **2018**, 367–427.

[21] M. S. Silva, *Molecules* **2017**, *22*, 247.

[22] T. T. Tidwell, *Tetrahedron* **1978**, *34*, 1855–1868.

[23] H. Aikawa, Y. Takahira, M. Yamaguchi, *Chem. Commun.* **2011**, *47*, 1479–1481.

[24] D. B. Amabilino, R. M. Kellogg, *Isr. J. Chem.* **2011**, *S1*, 1034–1040.

[25] R. S. Cahn, C. Ingold, V. Prelog, *Angew. Chemie Int. Ed. English* **1966**, *5*, 385–415.

[26] J. Vacek, L. Bednµrovµ, I. Císar, *Chem. – A Eur. J.* **2015**, *21*, 8910–8917.

[27] Y. Yamamoto, H. Sakai, J. Yuasa, Y. Araki, T. Wada, T. Sakanoue, T. Takenobu, T. Kawai, T. Hasobe, *Chem. – A Eur. J.* **2016**, *22*, 4263–4273.

[28] E. Weber, J. Ahrendt, S. Finge, I. Csöregh, M. Czugler, *J. Org. Chem.* **1988**, *53*, 5831–5839.

[29] I. Csoregh, S. Finge, E. Weber, *Bull. Chem. Soc. Jpn* **1991**, *64*, 1971–1975.

[30] S. Allenmark, U. Skogsberg, L. Thunberg, *Tetrahedron Asymmetry* **2000**, *11*, 3527–3534.

[31] H. Waldmann, M. Weigerding, C. Dreisbach, C. Wandrey, *Helv. Chim. Acta* **1994**, *77*, 2111–2116.

[32] H. J. Kreuzfeld, C. Dobler, *React. Kinet. Catal. Lett.* **1984**, *24*, 153–156.

[33] N. Jain, M. B. Mandal, A. V. Bedekar, *Tetrahedron* **2014**, *70*, 4343–4354.

[34] N. Jain, A. V. Bedekar, *Tetrahedron Asymmetry* **2011**, *22*, 1176–1179.

[35] N. Jain, A. V. Bedekar, *Tetrahedron Lett.* **2016**, *57*, 692–695.

[36] E. I. Kim, S. Paliwal, C. S. Wilcox, *J. Am. Chem. Soc.* **1998**, *120*, 11192–11193.